Re-Expression of Transcription Factor *ATF5* in Hepatocellular Carcinoma Induces G_2-M Arrest

Jennifer W-M. Gho,[1,2] Wai-Ki Ip,[1,2] Kathy Y-Y. Chan,[2] Priscilla T-Y. Law,[1,2] Paul B-S. Lai,[3] and Nathalie Wong[1,2]

[1]Li Ka-Shing Institute of Health Sciences, Departments of [2]Anatomical and Cellular Pathology and [3]Surgery, The Chinese University of Hong Kong, Shatin, Hong Kong, China

Abstract

Transcription factors represent an important class of genes that play key roles in controlling cellular proliferation, cell cycle modulation, and attractive targets for cancer therapy. Here, we report on the novel finding of common *ATF5* down-regulations in hepatocellular carcinoma (HCC), a highly malignant tumor with a dismal clinical course. Array-based mapping in HCC highlighted a high and consistent incidence of transcription factor *ATF5* repressions on regional chr.19q13. By quantitative reverse transcription-PCR, profound down-regulations of *ATF5* were further suggested in 78% of HCC tumors (60 of 77 cases) compared to their adjacent nontumoral liver ($P = 0.0004$). Restoration of *ATF5* expression in 3 nonexpressing HCC cell lines demonstrated a consistent growth inhibitory effect ($P < 0.029$) but minimal induction on cellular apoptosis. Subsequent flow cytometric investigations revealed a G_2-M cell cycle arrest in HCC cells that were ectopically transfected with *ATF5* ($P < 0.002$). The differential expressed genes from the functional effects of *ATF5* were examined by array profiling. Over a hundred genes were identified, among which *ID1* contains the *ATF/CREB* target binding sequences within its promoter region. An inverse relationship between *ATF5* expressions with *ID1* transcriptions was verified in HCC ($P = 0.019$), and a direct interaction of *ATF5* on the promoter of *ID1* was further demonstrated from electromobility shift assay. Examination of causal events underlying the silencing of *ATF5* in HCC suggested copy number losses, promoter hypermethylation, histone deacetylation, and DNA mutations to be the likely inactivating mechanisms. In conclusion, our finding supports a tumor suppressive role for *ATF5* in HCC, and highlighted *ID1* as a potential downstream target. [Cancer Res 2008; 68(16):6743–51]

Introduction

Hepatocellular carcinoma (HCC) is the 5th most common cancer worldwide and the 3rd most cause of cancer mortality (1). The overall dismal outcome of patients diagnosed with HCC is largely attributed to the tumor not being diagnosed in time for curative surgery. By the time of clinical presentation, most patients are at advanced inoperable stages, often with intrahepatic and extrahepatic metastases, which render surgical resection applicable to only a minority of patients (2). In addition, the high incidence of tumor recurrences, possibly from micrometastasis of tumor cells prior to curative surgery, further reduces patients' 5-year survival (3). Although the causative links of etiologic factors, including chronic hepatitis infections, heavy alcohol intake, dietary aflatoxin, and the male gender, in the development of HCC have been firmly established based on epidemiologic grounds (1), the molecular pathways by which HCC develops and progresses remain largely elusive. The recognition of reliable predictive biomarkers and a better understanding of biological pathway(s) by which HCC arises and progresses would undoubtedly provide directions for more efficacious therapies and improvements on overall patient prognosis.

Studies on the molecular pathogenesis of human cancers including breast, colon, prostate, and lung have guided the development of gene-based biomarkers and molecular-targeted therapies (4). In HCC, despite molecular investigations have indicated recurrent sites of genomic aberrations including regional amplicons, loss of heterozygosity, and cytogenetic translocations in the hepatic transformation from putative premalignant lesion of liver cirrhosis (5–7), few tumor suppressors and oncogenes have been defined within these causative loci. In this regard, recent advances in array-based transcriptional mapping offers the feasibility to correlate genomic aberrations with gene expression data. Such technological approach has allowed the unprecedented identification of candidate genes within casual sites of colorectal and invasive ductal breast carcinomas (8, 9).

By Spectral Karyotyping, we have previously reported on the novel presence of frequent nonreciprocal rearrangements of chr.19 in HCC, where abnormalities on 19q could be identified in as much as ~50% of primary tumors (7). Common chr.19q aberrations have also been described in a variety of human malignancies, including oligodendroglioma (10), astrocytoma (11), malignant gliomas (12), neuroblastoma (13), and ovarian carcinoma (14), where adverse prognostic associations have been further suggested in astrocytoma (11) and neuroblastoma (13). In prostate cancer, genome-wide linkage analysis has further suggested a susceptibility locus for a more aggressive tumor phenotype on chr.19q (12). Microsatellite analysis has defined the common deleted region to chr.19q13, where the presence of putative tumor suppressor gene(s) has long been speculated (11–13). Here, we describe an investigative study on the transcriptional activities of candidate genes on 19q in HCC. Using a high-resolution cDNA array, positional mapping indicated a high and consistent incidence of *Activating Transcription Factor 5* (*ATF5*; located on chr.19q13.3) down-regulations in HCC tumors and cell lines. The *ATF5* gene is a member of the *ATF/CREB* [cyclic AMP (cAMP)-dependent activating transcriptional factor/cAMP

Note: Supplementary data for this article are available at Cancer Research Online (http://cancerres.aacrjournals.org/).

J.W-M. Gho and W-K. Ip contributed equally to this work.

Requests for reprints: Nathalie Wong, Department of Anatomical and Cellular Pathology, The Chinese University of Hong Kong, Prince of Wales Hospital, Shatin, N.T., SAR Hong Kong, China. Phone: 852-2632-1128; Fax: 852-2637-6274; E-mail: natwong@cuhk.edu.hk.

doi:10.1158/0008-5472.CAN-07-6469

response element binding protein] family of transcription factors. The mammalian *ATF/CREB* family represents large groups of basic leucine zipper (bZIP) transcription factors with diverse physiologic functions that range from metabolite homeostasis to cellular differentiations and regulation of the cell cycle (13). Despite that the *ATF/CREB* family emerges as important cell survival factors, few studies have performed to characterize the *ATF5* gene in cancer. In this study, the functional influence of *ATF5* on HCC cell growth and its potential mechanistic actions were investigated. Our study highlighted a tumor suppressive role for *ATF5* in HCC and suggested *ID1*, an oncogenic transcription factor (15), as one of its transcriptionally regulated target.

Materials and Methods

Patients and cell lines. Tumorous liver tissues were collected from 87 patients who underwent curative surgery for HCC at Prince of Wales Hospital, Hong Kong. The corresponding adjacent nontumoral liver tissue was available for 77 patients. Informed consent was obtained from each patient recruited, and the study protocol was approved by the Clinical Research Ethics Committee of the Chinese University of Hong Kong. Among these 87 cases, patients' age ranged from 30 to 78 years (median age, 55 years) and a male to female ratio of 4.44 (71 males and 16 females). Patients were predominantly chronic HBV carriers (93%) with identifiable cirrhosis in the nontumorous liver indicated in 65 cases (75%) and histologic signs of chronic hepatitis suggested in 22 patients. The disease stage of tumors collected was classified according to the American Joint Committee on Cancer staging criteria (16), which graded 4 cases as stage I, 49 cases as stage II, 27 as stage III, and 7 as stage IV.

Eleven HCC cell lines (HKCI-1, HKCI-2, HKCI-3, HKCI-4, HKCI-7, HKCI-8, HKCI-9, HKCI-10, HKCI-C1, HKCI-C2, and HKCI-C3) were established from our laboratory and cultured as described previously (17–19). Hep3B, PLC/PRF/5, HepG2, Huh7, SNU387, SNU398, and SNU475 were cultured according to American Type Culture Collection recommendations. In the initial transcriptional mapping analysis by microarray, 10 randomly selected cell lines and 10 consecutive surgical HCC tumors were used. The array-derived finding on *ATF5* was first verified in the same set of array-analyzed specimens by quantitative reverse transcription-PCR (qRT-PCR). On establishing the common regulation of *ATF5* in these 20 specimens, further investigative analysis was conducted using the entire series of 87 HCC tumors, 77 adjacent nontumoral livers, and 18 cell lines.

Transcriptional mapping on Chr.19q. The expression array experiments were carried out as previously described (20). Briefly, differentially labeled Cy3 or Cy5 cDNA from cell line or primary HCC and normal liver pool were hybridized onto Human cDNA Arrays (Ontario Cancer Institute) that contained clones on chr.19q at a resolution of ~100 Kb. Hybridized images acquired were analyzed by GenePix Pro3.0 (Axon Instruments). Duplicate array hybridizations were performed for each tested sample. Custom Normalization Suite[4] was employed to integrate normalized signal ratios with physical map location of each cDNA clone.

qRT-PCR. Total RNA from cell lines, primary HCC, and adjacent nontumoral liver was subjected to first-strand cDNA synthesis using random hexanucleotide primer. Amplification of *ATF5* was performed using SYBR Green PCR (Applied Biosystems) with ACTB as internal reference gene. Primers for *ATF5* were 5′-GAGTGGCGACAGGATAGAGC-3′ (sense) and 5′-CCTCCCTCCCCTTAGCGTAGTGT-3′ (antisense), and the primers for ACTB were 5′-CGCGAGAAGATGACCCA GAT-3′ (sense) and 5′-GTACGGC-CAGAGGCGTACAG-3′ (antisense). Emission intensity from PCR assays was detected by the iCycler (BioRad Laboratories). Threshold cycles were averaged and expressed as a ratio relative to the mean value determined from seven normal human livers. Three adult human normal liver mRNAs were acquired from commercial companies (Ambion, Strategene, and CloneTech), and the remaining four normal livers were obtained from the colorectal cancer liver metastases, of which the liver at the surgical margin was histologically confirmed to be absent of underlying hepatic disease or cirrhosis. A ratio of <0.5 was considered down-regulation.

To allow analogous correlation between expressions of *ATF5* and downstream target *ID1* in later analysis, TaqMan assays targeting *ATF5* (Hs00247172_m1; Applied Biosystems), and *ID1* (NM_002165; sense, 5′-CTCTACGACATGAACGGCTGTT-3′; antisense, 5′-TGCTCACCT TGCG-GTTCTG-3′; probe, 5′-FAM-CACGCCTCAAGGAGCTGGTGCC-3′) were conducted. TaqMan assay for 18s (Hs99999901_s1) served as endogenous control.

Cell viability. Hep3B, HKCI-9, and HKCI-C1 seeded at 2×10^3 cells per well in 96-well culture plate were transfected with pcDNA3.1-ATF5 or pcDNA3.1-vector in Lipofectamine2000 (Invitrogen). Cell viability was measured every 24 h for 5 consecutive days by 3-(4,5-dimethylthiazol-2-yl)-2,5-diphenyltetrazolium bromide (MTT) assay. The absorbance of purple formazan was measured at 570 nm. Cell viability was expressed as a percentage of maximum absorbance from five replicates in three independent experiments. Transfected cells were also examined for apoptotic cells by fluorescence-based terminal deoxynucleotidyl-transferase–mediated dUTP nick-end labeling (TUNEL) or Annexin V assay.

Colony formation assay. pcDNA3.1-ATF5 and pcDNA3.1-vector–transfected Hep3B, HKCI-9, and HKCI-C1 cells were seeded at 2 to 4×10^4 per well in 6-well culture plate. After 2 to 4 wk of incubation in selective medium containing 1.5 mg/mL G418, colonies were fixed in 70% ethanol and stained by crystal violet. Visible colonies containing >50 cells were scored, and results from triplicate assays were expressed as a mean from 3 independent experiments.

Flow cytometry. HKCI-9 and Hep3B cell lines were stably transfected with either pcDNA3.1-ATF5 or pcDNA3.1-vector. Approximately 1×10^6 cells were cultured for 18 h in 6-well culture plate. Both floating and attached cells were collected, washed with PBS, and fixed in 70% cold ethanol for 1 h at −20°C. Fixed cells were incubated with RNase A and propidium iodide prior to flow cytometric analysis (BD FACSCalibur; Becton Dickinson).

Expression profiling. Hep3B cells transiently transfected with pcDNA3.1-ATF5 and geneticin-selected clone at 4th week were studied. Total RNA from transfectants and vector control was subjected to cRNA synthesis and hybridized onto CodeLink Human 20K-Bioarray (Amersham Biosciences). Signals captured by GenePix laser scanner (Axon) were analyzed by CodeLink Expression Analysis software. A differential gene expression was considered when a fold change was >2.0 or <0.5. Hierarchical clustering was performed by Eisen clustering and graphic presentation by Treeview.[5] Potential molecular pathways involved were examined by OntoExpress,[6] which utilizes information from the KEGG pathway database.

Immunofluorescence analysis. Transfected Hep3B cells with pEGFP-c2 and pEGFP-c2-ATF5 were seeded onto coverslips and cultured in complete medium for 24 h. Cells fixed with 4% paraformaldehyde were counterstained in 4′,6-diamidino-2-phenylindole (DAPI) and examined for *ATF5* subcellular location under a laser confocal microscope LSM5 PASCAL (Carl Zeiss).

Electrophoretic mobility shift assay. Hep3B cells transfected with either pEGFP-c2-ATF5 or pEGFP-c2 vector were extracted for nuclear proteins. Equal amounts of nuclear extracts were subjected to *ATF5* protein/DNA binding using the LightShift chemiluminescent EMSA (Pierce). A biotin end-labeled DNA oligo containing the CRE consensus sequence of the *ID1* promoter (5′-TTTATGAATGGGTGA CGTCACAGGCCTGGCG-3′) was incubated with the nuclear extracts or in combination with anti–green fluorescent protein (GFP) antibody. The DNA-protein and DNA-protein-antibody complexes were resolved on a 6% native PAGE and transferred to a Hybond-N+ membrane. Biotin end-labeled DNA was crosslinked onto the membrane, and detected using a streptavidin–horseradish peroxidase

[4] http://www.utoronto.ca/cancyto/

[5] http://rana.lbl.gov/EisenSoftware.htm

[6] http://vortex.cs.wayne.edu/ontoexpress/

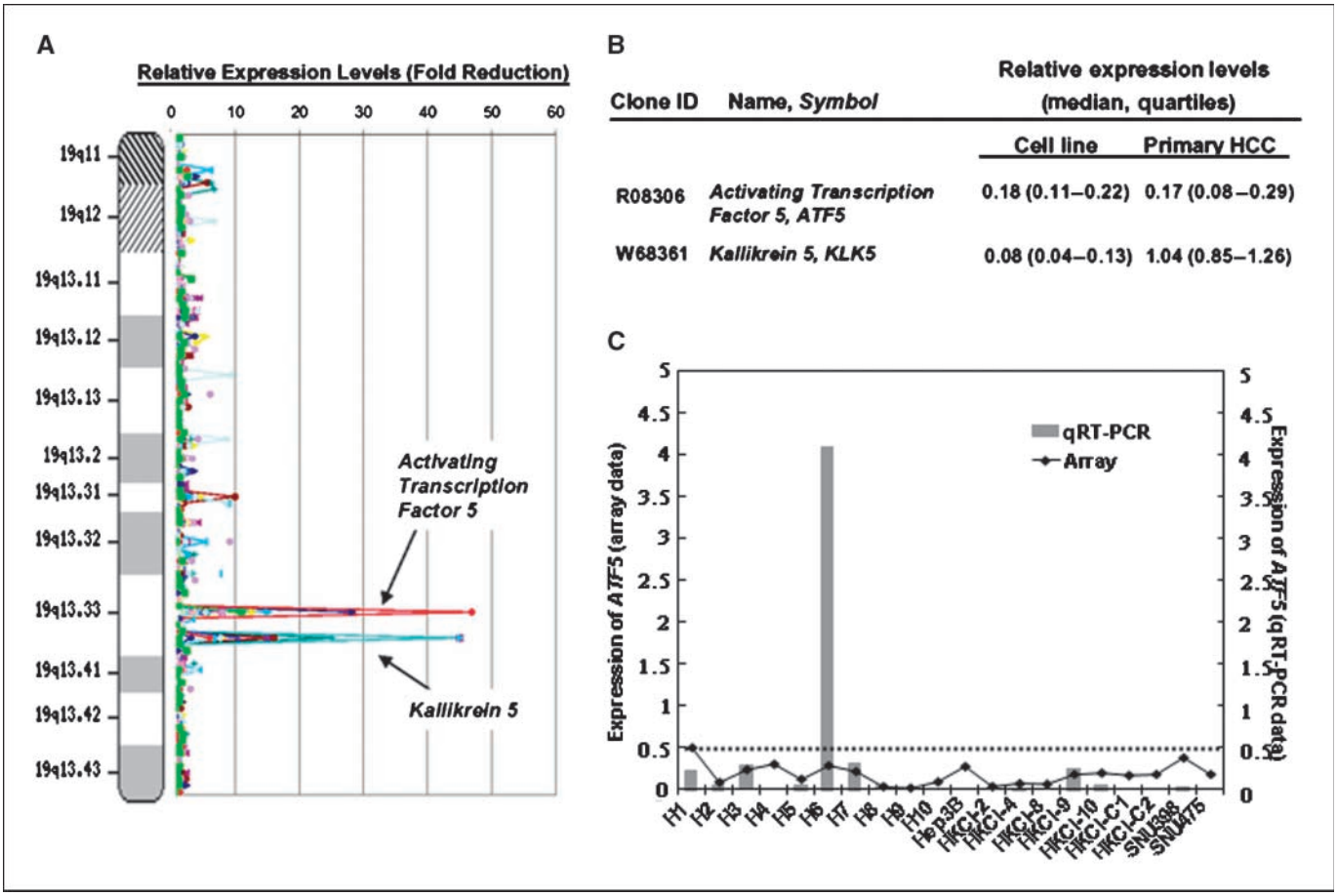

Figure 1. A transcript Map of Chr.19q in HCC. *A,* normalized gene expression levels of HCC tumors ($n = 10$) and cell lines ($n = 10$) have been plotted against physical map locations of cDNA clones in sequential order of megabases. *Inverted lines,* relative expression levels indicated substantial reduced expressions of clone R08306 representing the *ATF5* gene and clone W68361 representing *KLK5. B,* a consistent down-regulation of *ATF5* but not *KLK5* was suggested in both HCC tumors and cell lines. *C,* validative analysis by qRT-PCR on array-analyzed specimens suggested a concordant down-regulation of *ATF5* transcriptions in HCC tumors and cell lines, except for one tumor H6.

conjugate antibody and chemiluminescent substrate (GE Healthcare Bio-Sciences).

DNA sequencing. PCR amplifications of 5′untranslated region, exon 1 and exon 2, of *ATF5* gene were performed using primers designed at the introns exon boundary (Supplementary Table S1). The PCR product was subjected to BigDye Terminator Cycle Sequencing (Applied Biosystems) and analyzed on ABI PRISM3100. Sequence alignment was performed with the support of "Multiple Sequence Alignment with Hierarchical Clustering."[7] The data obtained from 23 HCC tumors and 18 cell lines was compared to 10 normal human livers.

Fluorescence *in situ* hybridization. Dual-color fluorescence in situ hybridization (FISH) was performed on 18 HCC cell lines as described (21). BAC RP11-510I16 containing *ATF5* and reference RP11-110A23 on chr.1p31.3 that seldom displays imbalances in HCC (5) were directly labeled with Spectrum Green-dUTP and Spectrum Orange-dUTP, respectively (Vysis). Counterstained in DAPI, each cell line was enumerated for hybridized signals in at least 50 interphase and metaphase cells.

5Aza-dC and TSA treatments. Six HCC cell lines, Hep3B, HKCI-2, HKCI-8, HKCI-9, HKCI-10, and HKCI-C1 were exposed to 5-Aza-2'-deoxycytidine (5Aza-dC) or TrichostatinA (TSA; Sigma-Aldrich) or a combination of both. For 5Aza-dC treatment, medium with 1 μmol/L 5Aza-dC was changed every 24 h for up to 72 h. For TSA treatment, cells were exposed to 300 nmol/L TSA for 24 h. In combinatory treatment, cells were treated with 1 μmol/L 5Aza-dC for 72 h followed by 300 nmol/L TSA for an additional 24 h. In parallel, untreated cells were cultured along with all conditions and served as control experiments. Cells were harvested for total RNA and examined for *ATF5* expression by qRT-PCR.

Bisulfitemodified DNA sequencing. Genomic DNA from HCC cell lines was chemically modified by bisulfite treatment using the CpGenome DNA Modification (Intergen). Approximately 1 μg DNA was denatured in 3 mol/L NaOH and processed according to manufacturer's instructions. Two CpG dense sites within 1,000 bp upstream from exon 1 were indicated in the promoter region of *ATF5*. The methylation pattern of these two CpG islands (island 1, −973 to −681; island 2, −132 to +219) relative to 3 normal livers was examined by direct sequencing of bisulfite modified DNA. Primer sequences for CpG island 1 were 5′-TGATAGTAGGTGTTGGATAGTTTAA-3′ (sense) and 5′-ACAAACCTTATACACAAAACTCAACTC-3′ (antisense), and the primer sequences for CpG island 2 were 5′-TTAGGA GGAGGAAATTA-GATTT-3′ (sense) and 5′-AAACTACAAAACCATAACC-3′ (antisense). Bisulfite-modified DNA at 100 ng was amplified with specific primers at annealing temperatures of 56°C for CpG island 1 and 54°C for CpG island 2. Freshly prepared PCR products were subcloned into pCR2.1-TOPO vector (Invitrogen). Ten colonies were selected from each sample. Nucleotide sequences of isolated plasmid DNA were determined on ABI PRISM3100 Genetic Analyzer after BigDye Terminator Cycle reaction.

Statistical analysis. Differences in *ATF5* expressions between HCC tumors and adjacent nontumoral liver were analyzed by the paired Student's t test. The Mann-Whitney U test was performed to evaluate the *ATF5* expression in the early and advanced stage tumors, between genders,

[7] http://prodes.toulouse.inra.fr/multalin/

and in specimens arising from chronic hepatitis and liver cirrhosis. Functional effects of *ATF5* in cell lines studied were assessed by Student's *t* test. Correlative analysis between *ATF5* and *ID1* expressions was performed by Pearson correlation. All data were expressed as mean ± SEM. Analysis was performed with SPSS and GraphPad Prism. A *P* value of <0.05 was considered significant.

Results

ATF5 expressions in HCC. Transcriptional mapping along chr.19q indicated two distinct down-regulated genes, *ATF5* and *KLK5*, both located on chr.19q13.33 (Fig. 1*A*). On further examination, reduced expressions of *KLK5* were observed only in cell lines, whereas down-regulations of *ATF5* were common in both cell lines and primary tumors (Fig. 1*B*). Validative analysis by qRT-PCR on the same array-analyzed specimens confirmed a concordant *ATF5* down-regulation, except for one case (Fig. 1*C*). The prevalence of *ATF5* repressions was further investigated in a cohort of HCC tumors and paired adjacent nontumoral liver. By qRT-PCR, a median expression of *ATF5* at a 0.12 and quartiles from 0.03 to 0.41 was suggested in 87 HCC compared to normal livers. When compared to their adjacent nontumoral liver (median, 1.22; quartiles, 0.39–3.05), *ATF5* appeared to be down-regulated in 78% of HCC (60 of 77 cases) by a median factor of 18-fold to >100-fold ($P = 0.0004$; Fig. 2*B*). Expressions of *ATF5* in the adjacent nontumoral livers were similar between chronic hepatitis and liver cirrhosis ($P = 0.88$; Fig. 2*A*). In HCC tumors, levels of *ATF5* expression did not show significant differences between early and advanced stage tumors, and between genders ($P > 0.09$; Fig. 2*C* and *D*).

Functional effects of ATF5. The functional influence of *ATF5* on cell growth was examined in three HCC cell lines, Hep3B, HKCI-9, and HKCI-C1, with negligible *ATF5* expressions. Ectopic expression of *ATF5* induced a consistent growth inhibitory effect in the three cell lines as assessed by colony formation and MTT assays (Fig. 3*A* and *B*). The growth attenuation by 30% to 50% was, however, not accompanied by a corresponding increase in apoptotic cells (Fig. 3*C*). The *ATF5*-induced growth suppression in Hep3B and HKCI-9 was further studied by flow cytometric analysis, which revealed a cell cycle arrest at the G_2-M phase in both cell lines ($P < 0.002$; Fig. 3*D*).

Potential regulatory pathways and modulated target ID1. The effect of *ATF5* on the transcriptional changes of Hep3B was investigated by gene expression profiling. In response to *ATF5* ectopic expression, transient and geneticin-selected stable transfectants showed a concordant up-regulation of 57 and down-regulation of 55 transcripts. Hierarchical clustering analysis of these 112 candidates depicted distinct cluster dendrograms of *ATF5* transfectants and vector controls (Fig. 4*A*). Bioinformatic analysis of 78 known genes from the 122 differential transcripts suggested few biological pathways including cell cycle, regulation of actin cytoskeleton, mitogen-activated protein kinase (MAPK) signaling, and focal adhesion that were likely modulated by *ATF5* (Table 1). In an effort to elucidate potential downstream targets of *ATF5*, the promoter region of 78 known genes was also examined for the presence of ATF/cAMP-responsive element binding protein (CREB) consensus binding sequences [TGACGT(C/A)(G/A); ref. 22]. Based on sequence information obtained from the University of California Santa Cruz database, four genes namely *ID1, RRAS,*

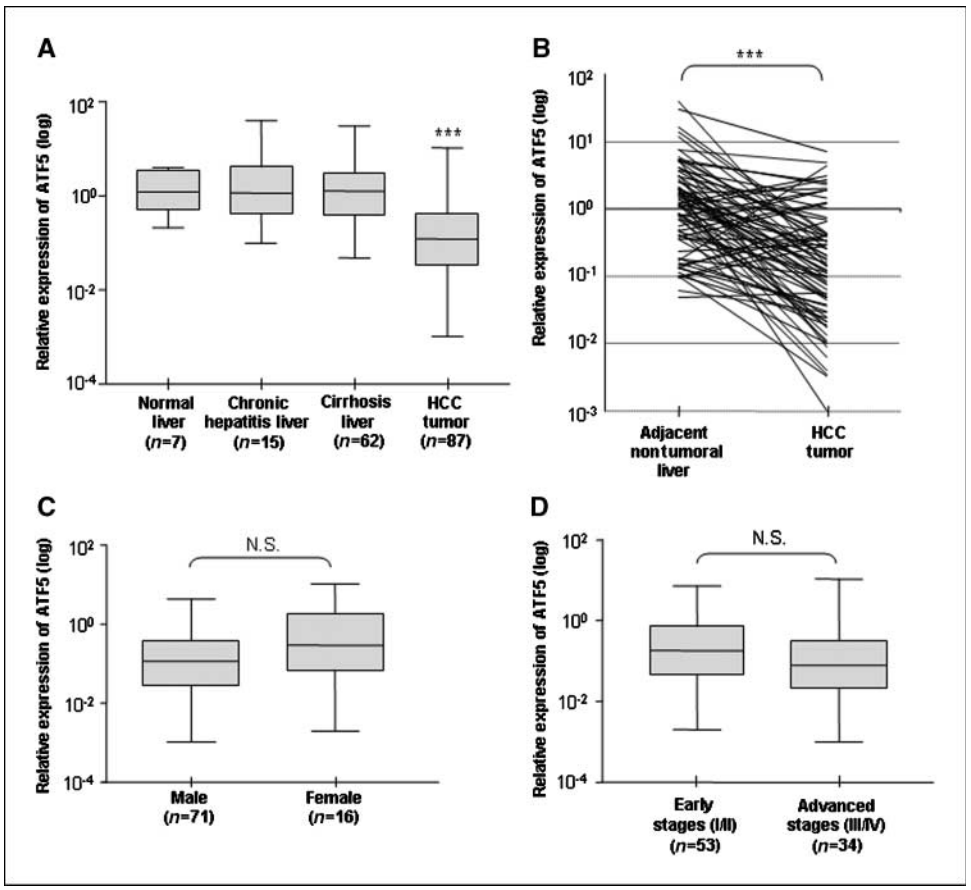

Figure 2. *ATF5* expression in HCC tumors and adjacent nontumoral liver. *A, ATF5* expressions in the adjacent nontumoral livers were similar between chronic hepatitis and liver cirrhosis ($P = 0.88$). Nevertheless, profound down-regulations of *ATF5* were found in the HCC tumors irrespective of a cirrhotic or chronic hepatitis background (Mann-Whitney *U* test; ***, $P < 0.0001$). *B,* qRT-PCR also indicated significant *ATF5* down-regulations in HCC tumors compared to their corresponding adjacent nontumoral liver ($n = 77$; paired *t* test; ***, $P = 0.0004$). *C* and *D,* differences in the *ATF5* expression were not suggested between gender ($P = 0.16$) nor between tumors of early and advanced stages ($P = 0.09$). *NS,* not significant.

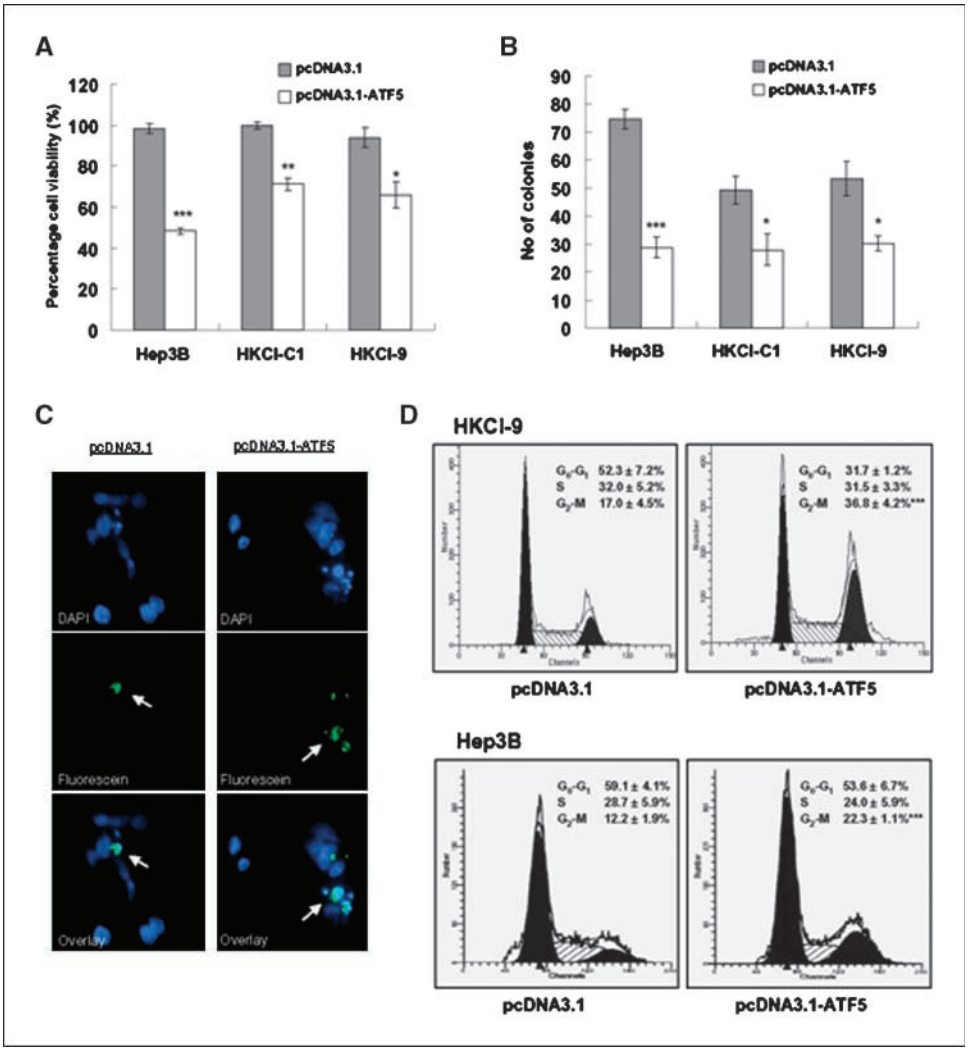

Figure 3. Functional effects of *ATF5*. *A,* ectopic transfection of pcDNA3.1-ATF5 in Hep3B, HKCI-C1, and HKCI-9 resulted in a consistent diminution on cell viability relative to vector control. *B,* colony formation assay suggested a significant growth inhibitory effect of restored *ATF5* expression on HCC cell lines. *C,* TUNEL assay did not indicate differences in the number of apoptotic cells (*white arrows*) between pcDNA3.1-ATF5 and pcDNA3.1-vector–transfected cells. *D,* the effect of *ATF5* on cell cycle profile was examined by flow cytometric analysis. A G_2-M cell cycle arrest was suggested in geneticin-selected clones of pcDNA3.1-ATF5 transfected HKCI-9 and Hep3B cells. *, $P < 0.05$; **, $P < 0.01$; ***, $P < 0.002$.

DUSP1, and *YWHAH* contain the consensus sequence in the proximity of their promoter region. The ATF/CREB consensus site in *ID1* and *RRAS* was found to locate before the transcription start site at −826bp and −1.6 kb, respectively, whereas in *YWHAH* and *DUSP1*, consensus sequence was located after the transcription start site at +71 bp and +46 bp, respectively. Because *ID1* harbors the ATF/CREB consensus site in the closest proximity and before the transcription start site, the possible interaction between *ATF5* and *ID1* was further investigated.

Down-regulation of *ID1* mRNA and protein in response to *ATF5* expression was confirmed in both transient and stable transfectants of Hep3B (Fig. 4*B*). An inverse relationship of *ATF5* mRNA transcribed with *ID1* expression levels was further established in HCC tumors and cell lines ($n = 35$; $r = -0.399$; $P = 0.019$; Fig. 4*C*). The potential direct interaction of *ATF5* with the ATF/CREB consensus binding site of *ID1* promoter was also examined by EMSA. Due to the lack of an effective antibody against *ATF5*, recombinant GFP–tagged vector pEGFP-c2-ATF5 was constructed and transfected into Hep3B cells with corresponding pEGFP-c2 vector as control. The GFP conjugated *ATF5* protein was found to localize predominantly in the nucleus, whereas vector control was contained within the cytoplasm (Fig. 4*D*). The nuclear extracts from the transfectants were subsequently subjected to EMSA analysis. As shown in Fig. 5*F*, a supershifted band suggestive of ATF5/DNA binding was detected in the pEGFP-c2-ATF5 transfectant with anti-GFP antibody. This band was found to disappear in the presence of unlabeled competitor oligo.

Inactivation mechanisms of ATF5. To investigate the possible underlying mechanisms in the inactivation of *ATF5*, mutational analysis, gene copy enumerations, and investigation of epigenetic changes had been carried out. Mutational analysis was conducted on 23 HCC tumors and 18 cell lines with varying expressions of *ATF5*. Despite a silent mutation that was suggested in the Hep3B cell line (Exon1 Leu30Leu), 3 somatic mutations were found in the primary tumors (7%, 3 of 41 cases). These mutations included Exon2 Leu141Phe, Exon2 Val257Met, and Exon2 Arg275Trp (Supplementary Table S1). According to qRT-PCR analysis, 2 mutated cases showed a down-regulation of *ATF5* by 2.6-fold and 8.1-fold as compared to normal livers, although the remaining case did not display aberrant expression. Enumeration of *ATF5* copy number by FISH analysis, on the other hand, indicated one or more copy loss in 11 of 18 HCC cell lines (61%), which included HKCI-1, HKCI-3, HKCI-8, HKCI-9, HKCI-C2, SNU387, SNU398, SNU475, PLC/PRF/5, Huh7, and HepG2 (Fig. 5*B*).

The possible involvement of epigenetic inactivation was investigated in 6 HCC cell lines (Hep3B, HKCI-C1, HKCI-2, HKCI-8, HKCI-9, and HKCI-10). Treatment with demethylating single agent 5Aza-dC indicated a re-expression of *ATF5* in 3 of 6 cell

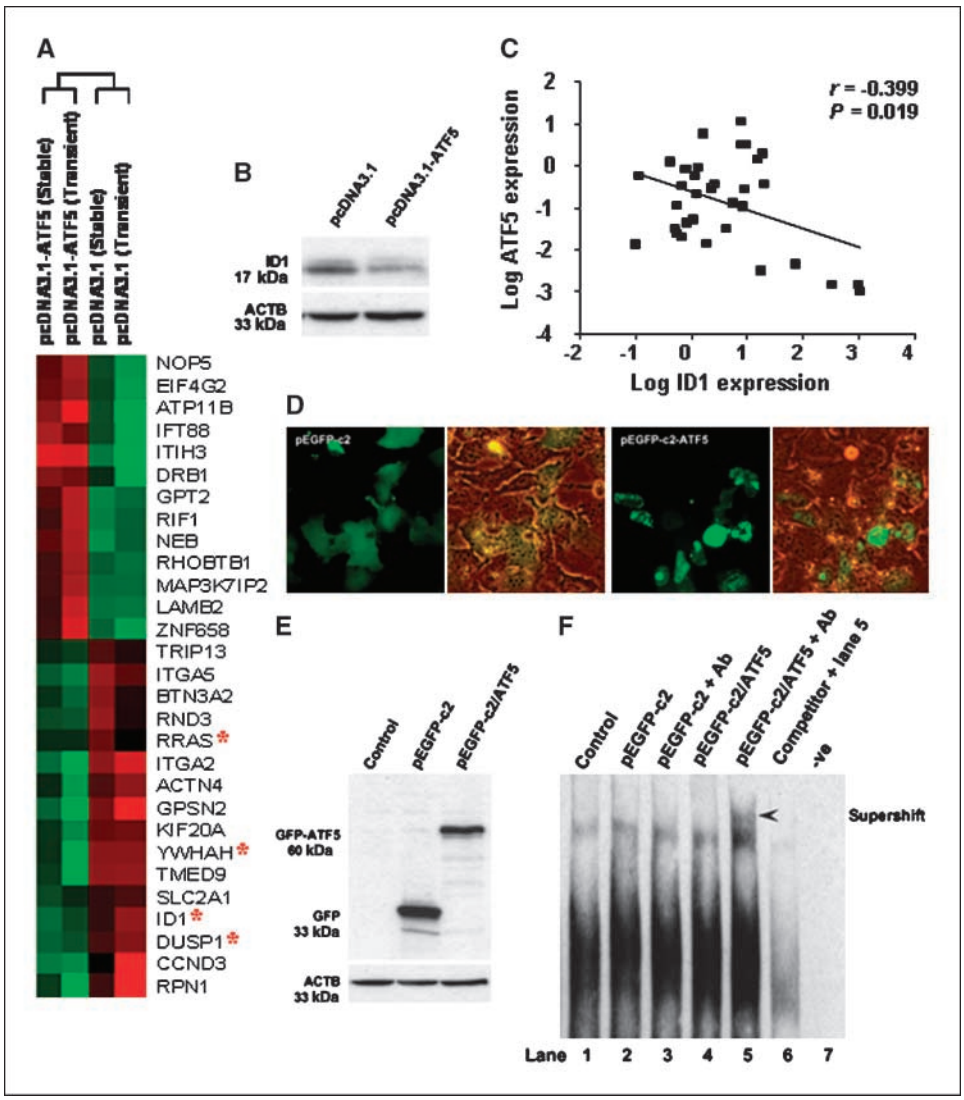

Figure 4. Identification of *ID1* as potential downstream target of *ATF5*. *A,* hierarchical clustering of 112 differential–expressed transcripts following *ATF5* transfections in Hep3B indicated 2 distinct dendrograms that coincided with transient and geneticin-selected pcDNA3.1-ATF5–transfected cells relative to vector controls. Genes containing the CRE consensus sequence in the proximity of their promoter region are highlighted (*). *B,* a reduced *ID1* protein translation following ectopic expression of *ATF5* was verified in Hep3B cells. *C,* an inverse relationship between *ATF5* expressions and *ID1* transcriptions was further established in an independent series of primary HCC tumors and cell lines. *D,* immunofluorescence analysis indicated predominant nuclear localization of GFP-tagged *ATF5* fusion protein, whereas pEGFP-c2 vector remained localized in the cytosol. *E,* translation of GFP-tagged *ATF5* fusion protein (60 kDa) in pEGFP-c2/ATF5–transfected Hep3B cells was confirmed. GFP protein (33 kDa) translated in pEGFP-c2 vector transfection is also shown. *F,* EMSA was performed using the nuclear extract containing GFP-ATF5 fusion protein and DNA oligos containing ATF consensus sequence. A supershifted band was detected with anti-GFP antibody (*Ab*) as shown in lane 5, suggesting that *ATF5* could directly interact with the CRE consensus binding site of *ID1* promoter.

lines (Hep3B, HKCI-C1, and HKCI-8; Fig. 5*A*). Although the use of histone deacetylase inhibitor TSA alone could not induce *ATF5* expressions in any cell lines, the combinatory application with 5Aza-dC was able to stimulate *ATF5* re-expressions in the three cell lines (HKCI-2, HKCI-9, and HKCI-10) that were unresponsive to single agent 5Aza-dC. Moreover, a synergistic action of both drugs led to an increased *ATF5* re-expression in HCKI-C1 and Hep3B by ~40-fold and ~5-fold, respectively, as indicated from qRT-PCR. Bisulfite sequencing of the 2 CpG dinucleotides regions of the *ATF5* promoter was conducted on Hep3B, HKCI-C1, HKCI-2, HKCI-8, HKCI-9, and HKCI-10. An increased methylation index between −794 to −688 of CpG island 1 was suggested in Hep3B, HKCI-C1, and HKCI-C1-8 compared to reference normal livers (Fig. 5*C*). Hypermethylation of CpG island 1 in the remaining three cell lines, however, was not suggested. According to the prediction of TESS,[8] a number of transcription factor binding sites including NF-E2, E-12, SP1, GC box, and hemoglobin was suggested on regional −794 to −688. For CpG island 2, despite its location being in closer proximity to the transcriptional start site, the methylation content was similar to normal liver controls in 6 of 6 cell lines examined.

Discussion

Transcription factors play essential roles in the control of normal cell physiology, and their alterations can lead to abnormalities in cell proliferation, differentiation, and survival. In many childhood acute leukemias, transcription factors have been altered through chromosomal translocations, resulting in their functional properties being either repressed or inappropriately activated. In this study, we have defined a novel transcription factor *ATF5* within the common aberrant region chr.19q13 of HCC. Frequent down-regulations of *ATF5* were found in HCC tumors (78%), and significant repressions from their putative premalignant lesion of liver cirrhosis and chronic hepatitis were also indicated (P = 0.0004). Although differences in the down-regulated levels with tumor progression was not suggested because *ATF5* is normally transcribed in the liver (23), our finding may have inference for *ATF5* down-regulations in the early transcriptional dysregulation contributory to the development of HCC.

[8] http://www.cbil.upenn.edu/cgi-bin/tess/tess

The *ATF5* gene belongs to the *ATF/CREB* family of bZIP proteins that control gene transcription through binding to the CRE consensus DNA sequence on the cellular promoter (20). Despite their diverse activities, *ATF/CREB* family members share a common ability in mediating cell signaling pathways and maintenance of cellular homeostasis. Furthermore, several *ATF* family members have been shown to be directly or indirectly involved in cell survival mechanisms. For example, *ATF2* have been reported to inhibit growth and metastasis (24). Ectopic expression of *B-ATF* has been shown to reduce the growth rate of murine cells (25). On the other hand, *ATF3* and *ATF4* appear to function as positive or negative regulators of cell viability depending on cellular context (26, 27). Although *ATF5* has been shown to play an essential role in the oligodendrocyte cell survival and neuronal progenitor cell differentiation (28, 29), the role(s) of *ATF5* in cancer pathogenesis remained largely undefined.

In this study, we demonstrated that restoration of *ATF5* expression in HCC cells resulted in growth inhibition through cell cycle arrest at the G_2-M phase (Fig. 3). Similar to other members of the *ATF/CREB* family, it would seem that *ATF5* also functions in the modulation of transcription networks involved in the cell cycle progression. To further explore the biological pathways and downstream target genes under the transcriptional control of *ATF5*, we performed gene expression profiling on *ATF5*–transfected HCC cells. Ectopic expression of *ATF5* induced >100 differential-expressed transcripts (Fig. 4). Informatic analysis of these differential genes suggested four regulatory pathways including cell cycle, actin cytoskeletal, MAPK signaling, and focal adhesion to be likely affected by *ATF5* (Table 1). In support of our finding, we found deregulated cell cycle genes, where the suppressed activities of YWHAH, an inhibitor of DNA damage–induced cell cycle arrest (30) and Cyclin D3, an interacting partner of a G_2-M–specific protein kinase, p58 (PITSLRE; ref. 31) may well have predisposed to the growth arrest observed. Although it is well-established that disruption of actin microtubule organization can induce G_2-M arrest (32), cooperative signaling between growth factor receptor tyrosine kinases, integrins, and the actin cytoskeleton is also fundamental to cell cycle progression (33). Under the transcriptional influence of *ATF5*, we found censored actin cytoskeleton regulation and focal adhesion pathway, where decreased expressions of major components such as *RRAS* and *EGFR* were found. Despite that *RRAS* has a high degree of sequence homology to *RAS*, unlike *RAS, RRAS* does not activate the MAPK pathway but rather elicits important integrin-dependent cellular behaviors such as adhesion and actin filamentous organizations

Table 1. Biological pathways modulated by ATF5

Pathways	Symbol	Gene name	Log2-fold induction
Cell cycle			
	ID1	Inhibitor of DNA binding 1	−1.68
	YWHAH	Tyrosine 3-monooxygenase/Tryptophan 5-monooxygenase Activation Protein, eta polypeptide	−1.97
	CCDN3	Cyclin D3	−1.82
	TGFB2	Transforming Growth Factor, β 2	−1.55
	RIF1	RAP1 Interacting Factor 1	1.19
Regulation of actin cytoskeleton			
	RRAS	Related RAS viral oncogene homologue	−1.19
	EGFR	Epidermal Growth Factor Receptor	−1.34
	ITGA5	Integrin, α 5	−1.98
	CSK	C-Src Tyrosine Kinase	−1.61
	ACTN4	Actinin, α 4	−1.65
	MSN	Moesin	−1.89
	MYO1C	Myosin IC	−1.08
	RND3	Rho Family GTPase 3	−1.64
	SFN	Stratifin	−1.63
MAPK signaling pathway			
	ID1	Inhibitor of DNA binding 1	−1.68
	DUSP1	Dual Specificity Phosphatase 1	−1.72
	EGFR	Epidermal Growth Factor Receptor	−1.34
	IL1B	Interleukin 1, β	−2.86
	TGFB2	Transforming Growth Factor, β 2	−1.55
	RPS6KA3	Ribosomal Protein S6 Kinase, polypeptide 3	1.26
	MAP3K7IP2	Mitogen-activated Protein Kinase Kinase Kinase 7 Interacting Protein 2	1.13
Focal adhesion			
	RRAS	Related RAS Viral Oncogene Homolog	−1.19
	ITGA5	Integrin, α 5	−1.98
	ACTN4	Actinin, α 4	−1.65
	EGFR	Epidermal Growth Factor Receptor	−1.34
	LAMB2	Laminin, β 2	1.27
	BIRC3	Baculoviral IAP Repeat-containing 3	−1.39

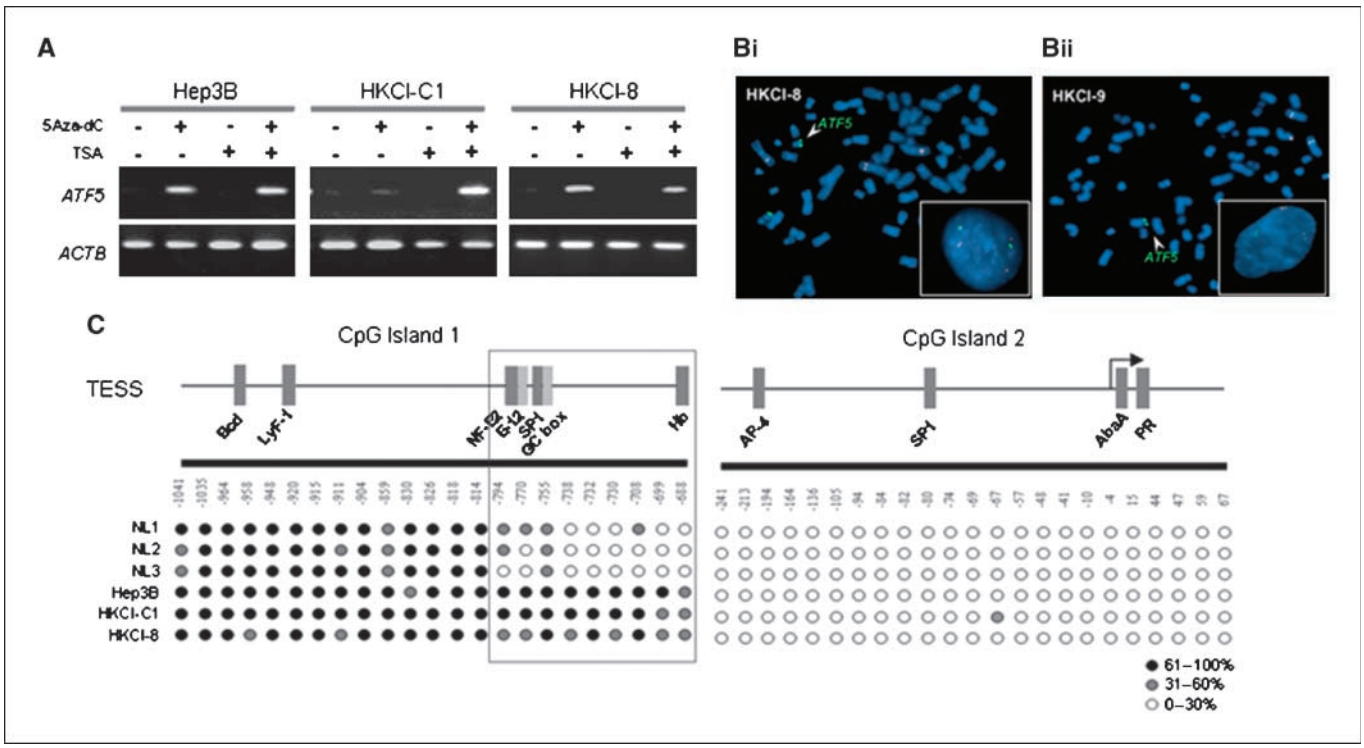

Figure 5. Inactivating mechanisms of *ATF5. A,* treatment with 5Aza-dC could induced re-expression of *ATF5* in HCC cell lines. A synergistic action with TSA was further suggested in HKCI-C1 and HKCI-8 as shown. *B,* dual-color FISH was performed with *ATF5* probe (*green*) and internal reference probe (*orange*). *Bi* and *Bii,* copy loss of *AFT5* in HKCI-8 and HKCI-9. *C,* bisulfite sequencing analysis on CpG islands 1 and 2 of *ATF5* promoter showed an increased methylation content within −794 to −688 (*in bracket*) of Hep3B, HKCI-C1, and HKCI-8 compared to normal livers (*NL*). Each circle represents methylation frequency from the analysis of 10 single clones.

(34). *EGFR*, on the other hand, can promote skin tumorigenesis through mitigating G_2-M arrest in UV-exposed keratinocytes (35). Thus, repressed genes expression and, thereof, the suppressed pathways resultant from *ATF5* restoration may have interfered with the transcriptional signaling network that normally regulates the cell cycle.

Studies on neural progenitor cells and oligodendrocyte precursor differentiations have implicated *ATF5* as a transcriptional repressor, which competes for binding to the CRE region (28, 29). In line with these findings, we found expressions of four CRE site–containing genes, namely *ID1, RRAS, YWHAH*, and *DUSP1*, to be repressed in response to ectopic *ATF5* expression. A reduced transcription of *ID1* mRNA and protein translated after *ATF5* transfection was verified *in vitro*, and an inverse relationship between *ATF5* and *ID1* expressions was further suggested in HCC tumors ($r = -0.399$; $P = 0.019$; Fig. 4*C*). Result from EMSA demonstrated the likelihood that *ATF5* could directly interact with *ID1* through the ATF/CRE consensus binding.

ID1 belongs to the helix-loop-helix family of transcription factors, and plays an important role as a signaling modulator of pathways involved in cellular developments, cell cycle progression, and neoplastic transformation (36). The level of *ID1* protein correlates significantly with both cancer progression and overall prognosis of a number of human malignancies (15). *ID1* is commonly overexpressed in HCC, where a functional role in the regulation of HCC cell growth and hepatic fibrogenesis has been suggested (37, 38). Increased expressions of *ID1* have also been implicated with increased risk of HCC development in patients with liver cirrhosis (38). Inhibition of *ID1* expression, on the other hand, could result in a suppressed cell proliferation possibly through the induction of cellular senescence and G_2-M cell cycle arrest (39). In prostate cancer, *ID1* is thought to exert its stimulatory effects through the activation of MAPK signaling pathway (40). Indeed, the MAPK pathway is also known to play an integral role in coordinating growth and survival signaling in the development and progression of HCC (41). Moreover, overexpression of intermediate proteins of MAPK pathway has been suggested in ~70% of HCC tumors (42). It is therefore plausible that repressed *ATF5* expression in HCC could result in the up-regulation of *ID1* and subsequent uncontrolled transcriptional activities, such as augmentation of MAPK signaling and inactivation of cell cycle checkpoint.

Studies on the possible inactivating mechanisms of *ATF5* suggested copy loss, promoter hypermethylation, histone modification, and DNA mutation in its common down-regulation in HCC. Of interest, a synergistic action of 5Aza-dC and TSA in the re-expression of *ATF5* was suggested in 5 of 6 HCC cell lines examined. This finding might hold therapeutic potentials for HCC patients, as clinical analogues of 5Aza-dC and TSA are currently available. The development of therapies that specifically target transcriptional factor abnormalities holds promise for improving outcome of diseases such as HCC that remains challenging to treat. Moreover, therapeutic strategies based on downstream target *ID1* might be effective given the clear relationship of *ID1* expression with cancer cell behaviors, and clinical outcomes in patient subgroups (31). Taken together, our present study highlighted a novel transcription factor *ATF5* in HCC. It is evident that much effort has still to be made to identify and

characterize molecular partners of *ATF5* protein, and to dissect the mechanism of *ATF5*-induced oncogenesis. A better understanding of *ATF5* partner proteins and associated pathways may potentially provide new options for therapeutic intervention in patients with HCC.

Disclosure of Potential Conflicts of Interest

No potential conflicts of interest were disclosed.

Acknowledgments

Received 12/4/2007; revised 4/24/2008; accepted 5/28/2008.

Grant support: Earmarked grants from the Hong Kong Research Grants Council (Ref. No.: CUHK 4289/04M) and, in part, supports from the Strategic Research, Chinese University of Hong Kong.

The costs of publication of this article were defrayed in part by the payment of page charges. This article must therefore be hereby marked *advertisement* in accordance with 18 U.S.C. Section 1734 solely to indicate this fact.

We thank Dr. Ben Beheshti and Prof. Jeremy Squire (University of Toronto, Canada) for their technical support in cDNA microarray analysis.

References

1. El-Serag HB, Rudolph KL. Hepatocellular carcinoma: epidemiology and molecular carcinogenesis. Gastroenterology 2007;132:2557–76.
2. Zhu AX. Hepatocellular carcinoma: Are we making progress? Cancer Invest 2003;21:418–28.
3. Poon RT, Fan ST, Lo CM, Liu CL, Wong J. Intrahepatic recurrence after curative resection of hepatocellular carcinoma: long-term results of treatment and prognostic factors. Ann Surg 1999;229:216–22.
4. Etzioni R, Urban N, Ramsey S, et al. The case for early detection. Nat Rev Cancer 2003;3:243–52.
5. Poon TC, Wong N, Lai PB, Rattray M, Johnson PJ, Sung JJ. A tumor progression model for hepatocellular carcinoma: bioinformatic analysis of genomic data. Gastroenterology 2006;131:1262–70.
6. Nagai H, Pineau P, Tiollais P, Buendia MA, Dejean A. Comprehensive allelotyping of human hepatocellular carcinoma. Oncogene 1997;14:2927–33.
7. Wong N, Lai P, Pang E, Leung TW, Lau JW, Johnson PJ. A comprehensive karyotypic study on human hepatocellular carcinoma by spectral karyotyping. Hepatology 2000;32:1060–8.
8. Staub E, Grone J, Mennerich D, et al. A genome-wide map of aberrantly expressed chromosomal islands in colorectal cancer. Mol Cancer 2006;5:37.
9. Reyal F, Stransky N, Bernard-Pierrot I, et al. Visualizing chromosomes as transcriptome correlation maps: evidence of chromosomal domains containing co-expressed genes-a study of 130 invasive ductal breast carcinomas. Cancer Res 2005;65:1376–83.
10. Zhu JJ, Santarius T, Wu X, et al. Screening for loss of heterozygosity and microsatellite instability in oligodendrogliomas. Genes Chromosomes Cancer 1998;21:207–16.
11. von Deimling A, Bender B, Jahnke R, et al. Loci associated with malignant progression in astrocytomas: a candidate on chromosome 19q. Cancer Res 1994;54:1397–401.
12. Rosenberg JE, Lisle DK, Burwick JA, et al. Refined deletion mapping of the chromosome 19q glioma tumor suppressor gene to the D19S412-STD interval. Oncogene 1996;13:2483–5.
13. Mora J, Cheung NK, Chen L, Qin J, Gerald W. Loss of heterozygosity at 19q13.3 is associated with locally aggressive neuroblastoma. Clin Cancer Res 2001;7:1358–61.
14. Bicher A, Ault K, Kimmelman A, Gershenson D, Reed E, Liang B. Loss of heterozygosity in human ovarian cancer on chromosome 19q. Gynecol Oncol 1997;66:36–40.
15. Perk J, Iavarone A, Benezra R. Id family of helix-loop-helix proteins in cancer. Nat Rev Cancer 2005;5:603–14.
16. Greene FL, American Joint Committee on Cancer, American Cancer Society. AJCC cancer staging manual. 6th/ed. New York: Springer-Verlag; 2002. xiv,421 ill.
17. Pang E, Wong N, Lai PB, To KF, Lau WY, Johnson PJ. Consistent chromosome 10 rearrangements in four newly established human hepatocellular carcinoma cell lines. Genes Chromosomes Cancer 2002;33:150–9.
18. Wong N, Chan KY, Macgregor PF, et al. Transcriptional profiling identifies gene expression changes associated with IFN-α tolerance in hepatitis C-related hepatocellular carcinoma cells. Clin Cancer Res 2005;11:1319–26.
19. Chan KY, Lai PB, Squire JA, et al. Positional expression profiling indicates candidate genes in deletion hotspots of hepatocellular carcinoma. Mod Pathol 2006;19:1546–54.
20. Persengiev SP, Green MR. The role of ATF/CREB family members in cell growth, survival and apoptosis. Apoptosis 2003;8:225–8.
21. Slager SL, Schaid DJ, Cunningham JM, et al. Confirmation of linkage of prostate cancer aggressiveness with chromosome 19q. Am J Hum Genet 2003;72:759–62.
22. Hai T, Hartman MG. The molecular biology and nomenclature of the activating transcription factor/cAMP responsive element binding family of transcription factors: activating transcription factor proteins and homeostasis. Gene 2001;273:1–11.
23. Su AI, Cooke MP, Ching KA, et al. Large-scale analysis of the human and mouse transcriptomes. Proc Natl Acad Sci U S A 2002;99:4465–70.
24. Bhoumik A, Huang TG, Ivanov V, et al. An ATP2-derived peptide sensitizes melanomas to apoptosis and inhibits their growth and metastasis. J Clin Invest 2002;110:643–50.
25. Echlin DR, Tae HJ, Mitin N, Taparowsky EJ. B-ATF function as a negative regulator of AP-1 mediated transcription and blocks cellular transformation by Ras and Fos. Oncogene 2000;19:1752–63.
26. Mashima T, Udagawa S, Tsuruo T. Involvement of transcriptional repressor ATF3 in acceleration of caspase protease activation during DNA damaging agent-induced apoptosis. J Cell Physiol 2001;188:352–8.
27. Tanabe M, Izumi H, Ise T, et al. Activating transcription factor 4 increases the cisplatin resistance of human cancer cell lines. Cancer Res 2003;63:8592–5.
28. Angelastro JM, Ignatova TN, Kukekov VG, et al. Regulated expression of ATF5 is required for the progression of neural progenitor cells to neurons. J Neurosci 2003;23:4590–600.
29. Mason JL, Angelastro JM, Ignatova TN, et al. ATF5 regulates the proliferation and differentiation of oligodendrocytes. Mol Cell Neurosci 2005;29:372–80.
30. Wanzel M, Kleine-Kohlbrecher D, Herold S, et al. Akt and 14–3-3eta regulate Miz1 to control cell-cycle arrest after DNA damage. Nat Cell Biol 2005;7:30–41.
31. Zhang S, Cai M, Zhang S, et al. Interaction of p58(PITSLRE), a G_2-M-specific protein kinase, with cyclin D3. J Biol Chem 2002;277:35314–22.
32. Sorger PK, Dobles M, Tournebize R, Hyman AA. Coupling cell division and cell death to microtubule dynamics. Curr Opin Cell Biol 1997;9:807–14.
33. Klein EA, Yung Y, Castagnino P, Kothapalli D, Assoian RK. Cell adhesion, cellular tension, and cell cycle control. Methods Enzymol 2007;426:155–75.
34. Self AJ, Caron E, Paterson HF, Hall A. Analysis of R-Ras signalling pathways. J Cell Sci 2001;114:1357–66.
35. Jean C, Hernandez-Pigeon H, Blanc A, Charveron M, Laurent G. Epidermal growth factor receptor pathway mitigates UVA-induced G_2-M arrest in keratinocyte cells. J Invest Dermatol 2007;127:2418–24.
36. Sikder HA, Devlin MK, Dunlap S, Ryu B, Alani RM. Id proteins in cell growth and tumorigenesis. Cancer Cell 2003;3:525–30.
37. Wiercinska E, Wickert L, Denecke B, et al. Id1 is a critical mediator in TGF-β-induced transdifferentiation of rat hepatic stellate cells. Hepatology 2006;43:1032–41.
38. Matsuda Y, Yamagiwa S, Takamura M, et al. Overexpressed Id-1 is associated with a high risk of hepatocellular carcinoma development in patients with cirrhosis without transcriptional repression of p16. Cancer 2005;104:1037–44.
39. Di K, Ling MT, Tsao SW, Wong YC, Wang X. Id-1 modulates senescence and TGF-β1 sensitivity in prostate epithelial cells. Biol Cell 2006;98:523–33.
40. Ling MT, Wang X, Ouyang XS, et al. Activation of MAPK signaling pathway is essential for Id-1 induced serum independent prostate cancer cell growth. Oncogene 2002;21:8498–505.
41. Farazi PA, DePinho RA. Hepatocellular carcinoma pathogenesis: from genes to environment. Nat Rev Cancer 2006;6:674–87.
42. Huynh H, Nguyen TT, Chow KH, Tan PH, Soo KC, Tran E. Over-expression of the mitogen-activated protein kinase (MAPK) kinase (MEK)-MAPK in hepatocellular carcinoma: its role in tumor progression and apoptosis. BMC Gastroenterol 2003;3:19.

Re-Expression of Transcription Factor *ATF5* in Hepatocellular Carcinoma Induces G_2-M Arrest

Jennifer W-M. Gho, Wai-Ki Ip, Kathy Y-Y. Chan, et al.

Cancer Res 2008;68:6743-6751.